

Supplementary Material

Supplementary Table 1. Relaxation delays for measuring T₁ and T₂ relaxation times¹

Relaxation delays			
T ₁ [ms] (pulse program hsqct1etf3gpsi.2)		T ₂ [ms] (pulse program hsqct2etf3gpsi)	
20	500	8.48	84.8
40	640	16.96	101.76
80	800	25.44	118.72
160	1200	33.92	135.68
250	1500	42.4	169.6
320	2000	50.88	203.52
		68.84	220.48
		137.44	

Supplementary Table 2. List of long-range NOE distance restraints obtained from a ^{15}N NOESY-HSQC experiment at 950 MHz used in CYANA calculations.

Res. Num.1	Res. Type	Atom	Res. Num. 2	Res. Type	Atom	max. dist (Å)
254	ALA	H	297	ALA	HB	5.00
258	LEU	H	293	ALA	HB	5.00
296	GLU	H	327	ALA	HA	5.50
298	GLN	H	297	ALA	H	5.00
343	ALA	HB	273	ARG	HG	5.00
290	ILE	H	258	LEU	HA	5.00
317	ALA	H	310	GLU	HG	5.00
304	ARG	HD	251	LEU	HD	6.00
300	LEU	H	248	LEU	HD	6.00
327	ALA	HA	296	GLU	HB	5.00
234	ARG	HD	247	ASP	HB	5.00
293	ALA	HB	261	LEU	HD	6.50
280	VAL	HG1	269	GLN	H	5.00
300	LEU	HA	251	LEU	HD	5.00
274	THR	H	339	SER	HA	5.00
293	ALA	H	261	LEU	HD	5.00
300	LEU	HG	324	VAL	HG2	5.50
261	LEU	HD	293	ALA	HA	5.00
258	LEU	HB	290	ILE	HD1	5.00
297	ALA	H	254	ALA	HB	5.00
290	ILE	HG2	261	LEU	HB	5.50
258	LEU	HA	290	ILE	HD1	5.00
300	LEU	HB	251	LEU	HD	5.00
297	ALA	HB	251	LEU	HD	5.00
251	LEU	HG	300	LEU	HA	5.00
251	LEU	HA	300	LEU	HA	5.50
280	VAL	HG1	268	ALA	HB	5.00
251	LEU	HG	300	LEU	H	5.00
272	HIS	HA	341	TRP	HE1	5.00

Supplementary Table 3. NMR and refinement statistics for protein structures

Protein	
NMR distance and dihedral constraints	
Distance constraints	
Total NOE	57
Intra-residue	0
Inter-residue	57
Sequential ($ i-j = 1$)	3
Medium-range ($ i-j < 4$)	18
Long-range ($ i-j > 5$)	36
Intermolecular	0
Hydrogen bonds	118
Total dihedral angle restraints	136
ϕ	68
ψ	68
Structure statistics	
Violations (mean and s.d.)	
Distance constraints (Å)	0.068 ± 0.0086
Dihedral angle constraints (°)	0
Max. dihedral angle violation (°)	0
Max. distance constraint violation (Å)	2.1
Deviations from idealized geometry	
Bond lengths (Å)	0.001
Bond angles (°)	0.2
Average pairwise r.m.s. deviation** (Å)	
Heavy	0.7
Backbone	1.4

**Pairwise r.m.s. deviation was calculated among 20 refined structures.

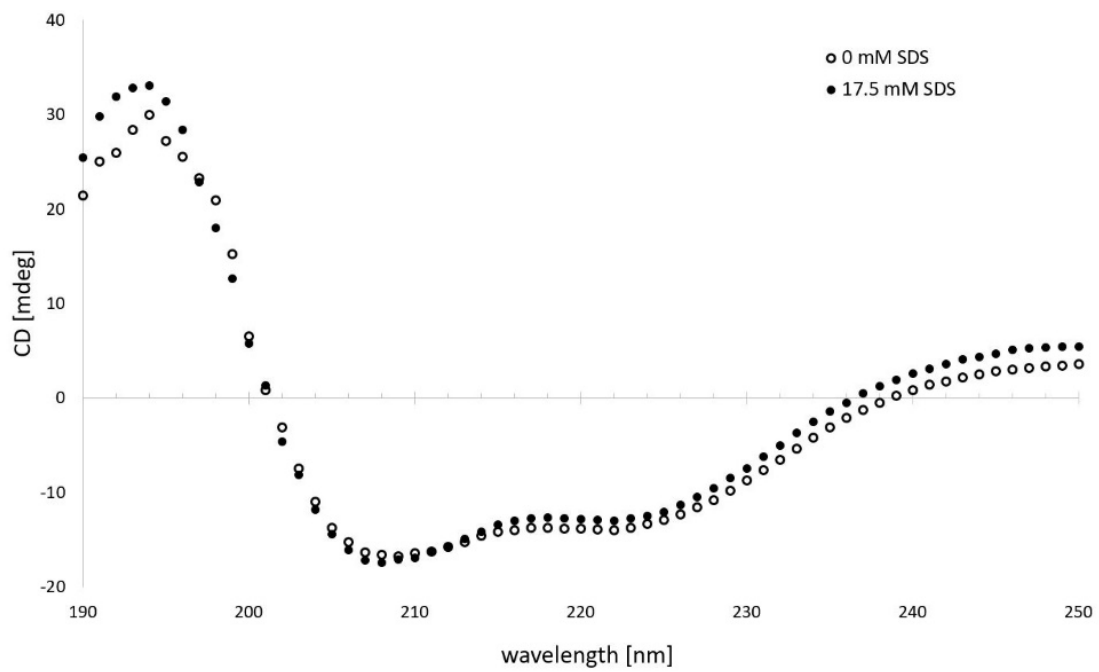
Supplementary Table 4. Exact p values for statistical analyses in Figure 4 using Student's two-tailed t-test.

Figure 4a					
Left			Right		
Comparison	p Value 190 s	p Value 230 s	Comparison	p Value 0 s	p Value 190 s
WT vs. I290S + A293S	0.03418	0.23389	WT vs. I290S + A293S	0.22306	0.03418
WT vs. I290S + A293S + R304W	0.24246	0.3214	WT vs. I290S + A293S + R304W	0.54922	0.24247
WT vs. R304W	0.91754	0.9666	WT vs. R304W	8.13188E-20	0.91755
I290S + A293S vs. I290S + A293S + R304W	0.0029	0.0436	I290S + A293S vs. I290S + A293S + R304W	0.54753	0.0029
I290S + A293S vs. R304W	0.01996	0.23038	I290S + A293S vs. R304W	5.67997E-19	0.01996
I290S + A293S + R304W vs. R304W	0.27889	0.35313	I290S + A293S + R304W vs. R304W	2.86134E-17	0.27889

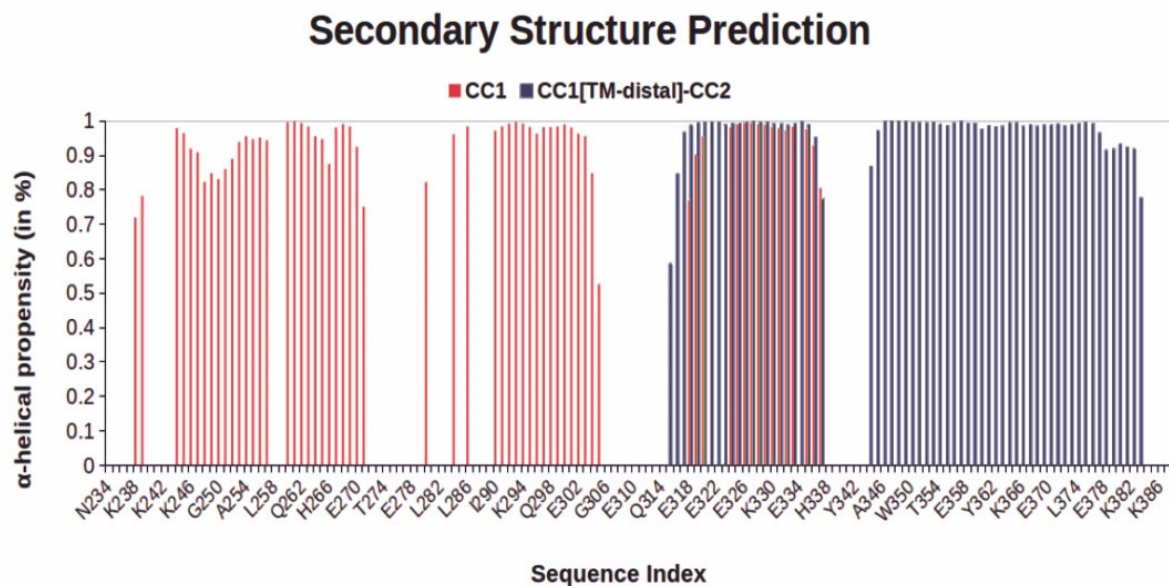
Figure 4b					
Left			Right		
Comparison	p Value 190 s	Comparison	p Value 0 s	p Value 190 s	
WT vs. L300S + L303S	0.00605	WT vs. L300S + L303S	0.50748	0.00605	
WT vs. L300S + L303S + R304W	0.0098	WT vs. L300S + L303S + R304W	0.1163	0.0098	
WT vs. R304W	0.3108	WT vs. R304W	3.57135E-13	0.31079	
L300S + L303S vs. L300S + L303S + R304W	0.77911	L300S + L303S vs. L300S + L303S + R304W	0.33739	0.77911	
L300S + L303S vs. R304W	0.02982	L300S + L303S vs. R304W	2.81665E-12	0.02982	
L300S + L303S + R304W vs. R304W	0.05119	L300S + L303S + R304W vs. R304W	2.81664E-12	0.05119	

Supplementary Table 5. Exact p values for statistical analyses in Figure 5 using Student's two-tailed t-test.

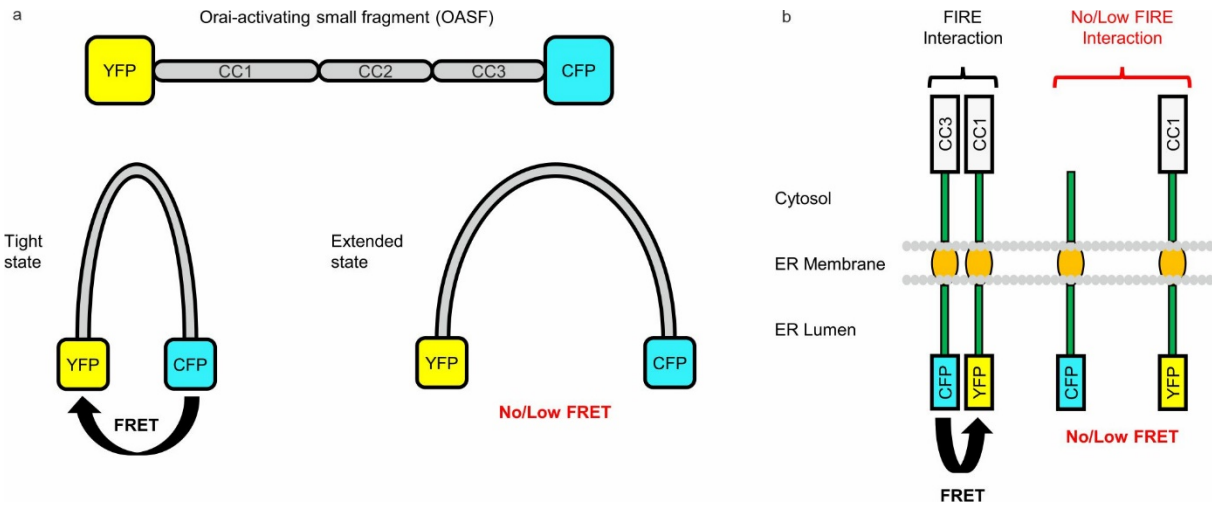
Figure 5a		Figure 5b		Figure 5c	
Comparison	p Value	Comparison	p Value	Comparison	p Value
WT vs. I290S + A293S	5.31461E-7	WT PM vs. Cyto	4.55539E-6	WT vs. I290S + A293S	2.22052E-4
WT vs. I290S + A293S + R304W	2.89604E-11	I290S + A293S PM vs. Cyto	2.04509E-5	WT vs. I290S + A293S + R304W	0.0073
WT vs. R304W	3.24268E-28	I290S + A293S + R304W PM vs. Cyto	1.11904E-7	WT vs. R304W	0.98932
I290S + A293S vs. I290S + A293S + R304W	0.12731	R304W PM vs. Cyto	0.45371	I290S + A293S vs. I290S + A293S + R304W	0.11358
I290S + A293S vs. R304W	5.7787E-22			I290S + A293S vs. R304W	2.74836E-4
I290S + A293S + R304W vs. R304W	3.10574E-25			I290S + A293S + R304W vs. R304W	0.01746
Figure 5d		Figure 5e		Figure 5f	
Comparison	p Value	Comparison	p Value	Comparison	p Value
WT vs. L300S + L303S	1.67348E-21	WT PM vs. Cyto	8.33265E-6	WT vs. L300S + L303S	0.01807
WT vs. L300S + L303S + R304W	9.24136E-32	L300S + L303S PM vs. Cyto	6.35422E-4	WT vs. L300S + L303S + R304W	0.04448
WT vs. R304W	2.0318E-76	L300S + L303S + R304W PM vs. Cyto	9.74467E-4	WT vs. R304W	0.86454
L300S + L303S vs. L300S + L303S + R304W	0.01997	R304W PM vs. Cyto	0.32921	L300S + L303S vs. L300S + L303S + R304W	0.75196
L300S + L303S vs. R304W	5.59361E-53			L300S + L303S vs. R304W	0.00984
L300S + L303S + R304W vs. R304W	1.73199E-54			L300S + L303S + R304W vs. R304W	0.02697



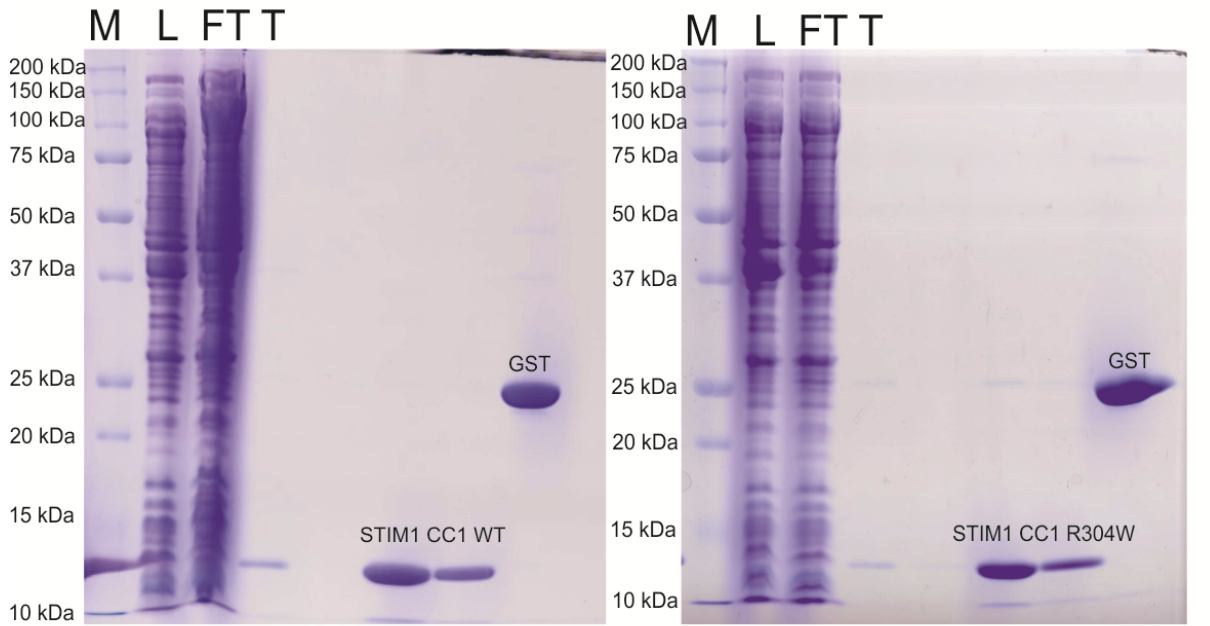
Supplementary Fig. 1 The CD spectra of 40 μ M STIM1 CC1 WT without (open black circles) and after addition (close black circles) of 17.5 mM (0.5%) SDS detergent.



Supplementary Fig. 2. TalosN² secondary structure predictions for CC1 STIM1 and previously published CC1_[TM-distal]-CC2 STIM1 fragments.³



Supplementary Fig. 3. (a) YFP-OASF-CFP conformational sensor primary structure together with simplified depictions of a tight (intramolecular FRET) and an extended state (No/Low intramolecular FRET). **(b)** Schematic representation of the FIRE system showing how intermolecular FRET is occurring. A control experiment lacking FIRE interaction is indicated on the right.

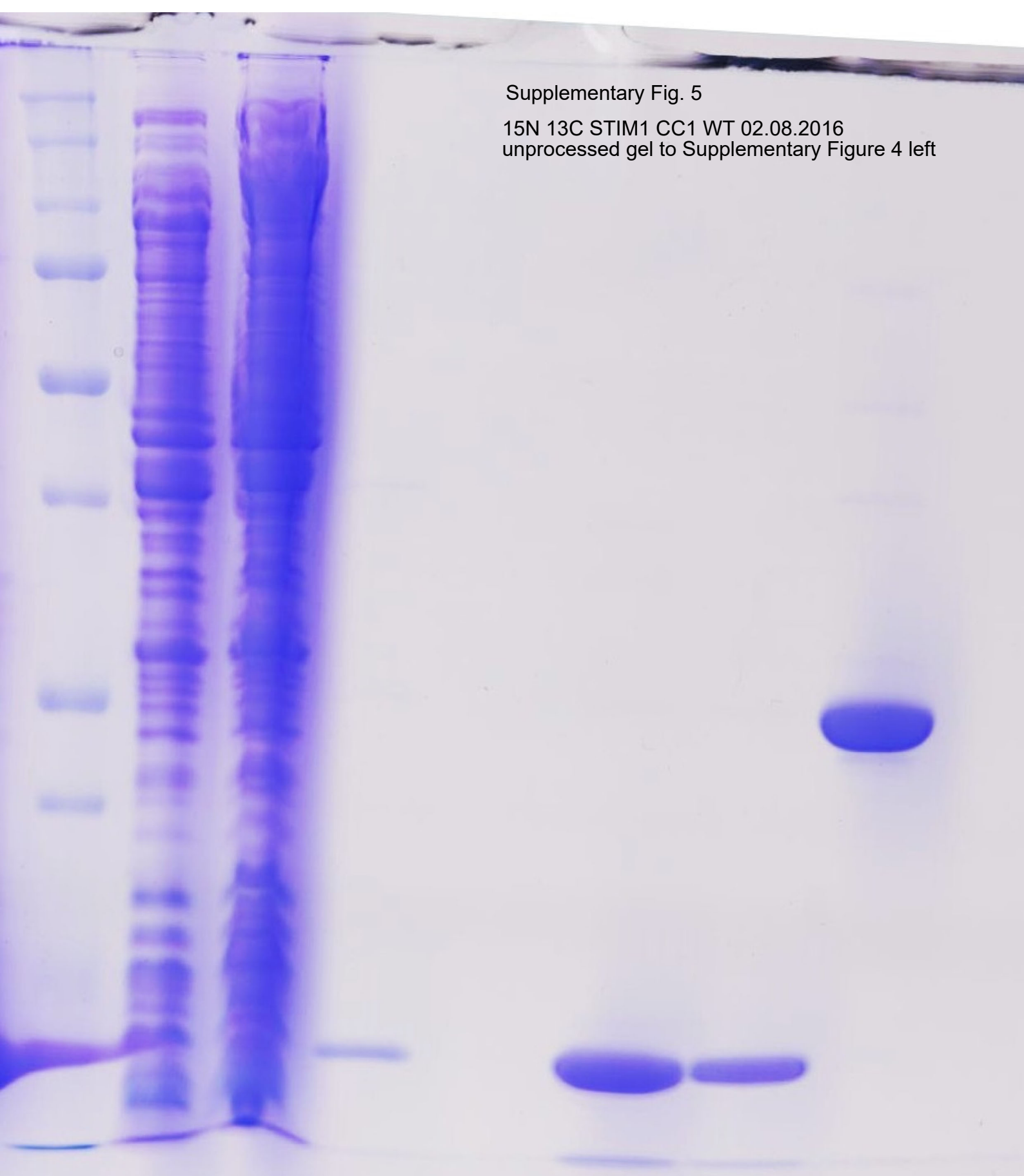


Supplementary Fig. 4. SDS-PAGE monitoring of STIM1 CC1 WT (left) and R304W (right) purifications. M – molecular marker, L – crude lysate (GST-CC1 fusion~ 37 kDa). FT – flow through fraction, T – losses during the on-column thrombin cleavage, GST – cleaved GST-tag. The protein samples were expressed and purified according to our previously published protocol.⁴ Each gel has been repeated at least 5 times with independent preparations.

1. Palmer AG, 3rd. Nmr probes of molecular dynamics: overview and comparison with other techniques. *Annual review of biophysics and biomolecular structure* **30**, 129-155 (2001).
2. Shen Y, Bax A. Protein backbone and sidechain torsion angles predicted from NMR chemical shifts using artificial neural networks. *Journal of Biomolecular NMR* **56**, 227-241 (2013).
3. Stathopoulos PB, *et al.* STIM1/Orai1 coiled-coil interplay in the regulation of store-operated calcium entry. *Nat Commun* **4**, 2963 (2013).
4. Rathner P, Stadlbauer M, Romanin C, Fahrner M, Derler I, Müller N. Rapid NMR-scale purification of ^{(15)N},^{(13)C} isotope-labeled recombinant human STIM1 coiled coil fragments. *Protein Expr Purif* **146**, 45-50 (2018).

Supplementary Fig. 5

15N 13C STIM1 CC1 WT 02.08.2016
unprocessed gel to Supplementary Figure 4 left



Supplementary Fig. 6

15N 13C STIM1 CC1 R304W 07.07.2016
unprocessed gel to Supplementary Figure 4 right

